

Geometric and Operational Characterization of Two-Qutrit Entanglement

Ankita Jana

Department of Physics, Indian Institute of Technology Jammu, Jammu,
181221, Jammu & Kashmir, India

Abstract

We investigate the entanglement structure of bipartite two-qutrit pure states from both geometric and operational perspectives. Using the eigenvalues of the reduced density matrix, we analyze how symmetric polynomials characterize pairwise and genuinely three-level correlations. We show that the determinant of the coefficient matrix defines a natural, rank-sensitive geometric invariant that vanishes for all rank-2 states and is nonzero only for rank-3 entangled states. An explicit analytic constraint relating this determinant-based invariant to the I-concurrence is derived, thereby defining the physically accessible region of two-qutrit states in invariant space. Furthermore, we establish an operational correspondence with three-path optical interferometry and analyze conditional visibility and predictability in a qutrit quantum erasure protocol, including the effects of unequal path transmittances. Numerical demonstrations confirm the analytic results and the associated complementarity relations. These findings provide a unified geometric and operational framework for understanding two-qutrit entanglement.

Keywords: Two-qutrit entanglement; I-concurrence; Determinant invariant; Symmetric polynomials; Quantum erasure; Multi-path interferometry

1 Introduction

Higher-dimensional quantum systems offer a substantially richer set of correlation structures compared to two-level systems and therefore play an increasingly important role in quantum information science [1]. In particular, qutrit-based architectures have attracted considerable interest due to their potential advantages in quantum communication, including enhanced security, increased information capacity, and improved resilience to noise [2–4]. These features motivate a detailed investigation of entanglement properties in higher-dimensional bipartite systems.

For bipartite pure states, entanglement is fully determined by the spectral properties of the reduced density matrix obtained by tracing out one subsystem [1, 5]. In two-level systems, this spectral characterization underlies standard entanglement quantifiers such as concurrence [5] and entanglement of formation. In contrast, higher-dimensional systems exhibit additional correlation structures that cannot be described solely in terms of two-level coherence. In the case of two-qutrit states, the presence of three non-negative eigenvalues naturally allows one to distinguish between correlations arising from pairwise combinations of levels and those involving all three levels simultaneously [5, 6].

Despite extensive progress in the development of entanglement measures and invariant-based classifications for higher-dimensional systems, a comprehensive geometric and algebraic understanding of two-qutrit entanglement remains incomplete. In particular, the interplay between the rank of the reduced density matrix, the internal structure of the coefficient matrix describing the state, and

the connection between abstract entanglement invariants and experimentally accessible quantities has not yet been fully clarified within a unified framework [7, 8].

Beyond spectral information alone, the algebraic structure of a bipartite quantum state is encoded in its coefficient matrix. The cofactor structure of this matrix is directly related to the eigenvectors of the reduced density matrix, indicating a deeper relationship between matrix algebra, symmetric polynomials of the eigenvalues, and entanglement properties[7]. Exploring this relationship provides a natural route toward identifying geometric invariants that distinguish different forms of entanglement in two-qutrit systems [7, 8].

While determinant-based invariants and concurrence-type measures have been investigated independently in the context of higher-dimensional entanglement, a direct analytic and geometric comparison between a determinant-based invariant and the I-concurrence for two-qutrit pure states has not been explicitly explored, to the best of our knowledge [5, 9, 10].

In this work, we present a unified geometric and operational characterization of entanglement in bipartite two-qutrit pure states, building on existing concurrence-based measures and invariant approaches[5, 6, 9]. Using symmetric polynomials of the eigenvalues of the reduced density matrix, we separate contributions associated with pairwise correlations from those arising from genuinely three-level entanglement. We show that the determinant of the coefficient matrix defines a natural, rank-sensitive geometric invariant that vanishes for all rank-2 states and becomes nonzero only for rank-3 entangled states. An explicit analytic constraint relating this determinant-based invariant to the I-concurrence is derived, thereby delineating the physically accessible region of two-qutrit states in invariant space.

Furthermore, we establish an operational interpretation of the geometric invariants through a correspondence with three-path optical interferometry. Within this framework, we analyze conditional visibility and predictability in a qutrit quantum erasure protocol, including the effects of unequal path transmittances. Numerical simulations are used to validate the analytic results and the associated complementarity relations. Together, these results provide a unified geometric and operational perspective on two-qutrit entanglement [11–13].

2 Theoretical Background

We consider a bipartite quantum system composed of two qutrits, described within a $3 \otimes 3$ Hilbert space. Any pure state of this composite system can be expressed in the computational basis as

$$|\Psi\rangle = \sum_{i,j=1}^3 C_{ij} |i\rangle_A |j\rangle_B, \quad (1)$$

where C is a complex 3×3 coefficient matrix and $\{|i\rangle_A\}$ and $\{|j\rangle_B\}$ denote orthonormal bases for subsystems A and B , respectively. Throughout this work, the state is assumed to be normalized.

The reduced state of subsystem A is obtained by tracing over subsystem B , leading to the reduced density matrix

$$\rho_A = \text{Tr}_B(|\Psi\rangle\langle\Psi|), \quad (2)$$

which can be written explicitly in terms of the coefficient matrix as

$$\rho_A = CC^\dagger, \quad \text{Tr}(\rho_A) = 1. \quad (3)$$

The matrix ρ_A is Hermitian, positive semidefinite, and normalized to unit trace. Its eigenvalues $\{\lambda_1, \lambda_2, \lambda_3\}$ therefore satisfy

$$\lambda_1 + \lambda_2 + \lambda_3 = 1. \quad (4)$$

For bipartite pure states, the entanglement properties are fully determined by the eigenvalue spectrum [1, 5].

For higher-dimensional bipartite systems, several entanglement measures have been proposed to generalize the notion of concurrence beyond two-level systems. Among these, the I-concurrence provides a natural extension applicable to arbitrary finite dimensions [5]. For a two-qutrit pure state, the I-concurrence is defined as

$$C_I = \sqrt{2(1 - \text{Tr } \rho_A^2)} = 2\sqrt{\lambda_1\lambda_2 + \lambda_2\lambda_3 + \lambda_3\lambda_1} = 2\sqrt{s_2}. \quad (5)$$

Invariant-based approaches and algebraic characterizations of entanglement in higher-dimensional systems have also been explored in the literature [6, 7]. For a maximally entangled two-qutrit pure state $\lambda_1 = \lambda_2 = \lambda_3 = \frac{1}{3}$, the I-concurrence attains its maximum value

$$C_I^{\max} = \frac{2}{\sqrt{3}}. \quad (6)$$

This form makes explicit that the I-concurrence depends solely on pairwise products of the eigenvalues and therefore captures correlations associated with two-level coherences within the qutrit system.

Beyond spectral properties, the algebraic structure of the coefficient matrix C plays an important role in determining the properties of ρ_A . A useful identity for any 3×3 matrix M is

$$(M - \lambda I) \text{adj}(M - \lambda I) = \det(M - \lambda I) I \quad (7)$$

where $\text{adj}(\cdot)$ denotes the adjugate matrix [7]. For an eigenvalue $\lambda = \lambda_i$ of ρ_A , the determinant vanishes, implying

$$(\rho_A - \lambda_i I) \text{adj}(\rho_A - \lambda_i I) = 0. \quad (8)$$

As a consequence, the columns of the adjugate matrix provide eigenvectors of ρ_A . This establishes a direct connection between the cofactor structure of the coefficient matrix C and the eigenstructure of the reduced density matrix[7, 8].

The eigenvalues of ρ_A also define three elementary symmetric polynomials,

$$s_1 = \lambda_1 + \lambda_2 + \lambda_3 = 1, \quad s_2 = \lambda_1\lambda_2 + \lambda_2\lambda_3 + \lambda_3\lambda_1, \quad s_3 = \lambda_1\lambda_2\lambda_3. \quad (9)$$

While s_2 quantifies pairwise correlations and directly determines the I-concurrence[5, 6], the third-order polynomial s_3 captures genuinely three-level correlations that are absent in rank-2 states[7]. This observation motivates the introduction of a rank-sensitive geometric invariant, developed in the following section.

3 Symmetric Polynomial Geometry and Rank Structure

The spectrum $\{\lambda_1, \lambda_2, \lambda_3\}$ of the reduced density matrix provides a natural geometric characterization of two-qutrit entanglement through the elementary symmetric polynomials. Since the trace is fixed by normalization, $s_1 = \lambda_1 + \lambda_2 + \lambda_3 = 1$, the entanglement properties are fully determined by the remaining two independent invariants s_2 and s_3 [1, 7]:

$$s_2 = \lambda_1\lambda_2 + \lambda_2\lambda_3 + \lambda_3\lambda_1, \quad s_3 = \lambda_1\lambda_2\lambda_3. \quad (10)$$

The second-order polynomial s_2 quantifies correlations arising from pairwise combinations of the Schmidt components and directly determines the I-concurrence, as discussed above [5, 6]. In

contrast, the third-order polynomial s_3 captures correlations that involve all three levels simultaneously and therefore represents genuinely three-level entanglement [7].

A particularly important consequence of this structure is its sensitivity to the rank of the reduced density matrix. Rank-2 states are characterized by the vanishing of one eigenvalue, which implies

$$s_3 = 0, \quad (11)$$

whereas rank-3 states satisfy $s_3 > 0$, reflecting the presence of correlations across all three levels. The polynomial s_3 therefore acts as a sharp indicator of the rank of the entangled state and provides a natural geometric separation between pairwise and genuinely three-level correlations in two-qutrit systems [7, 8].

This rank sensitivity admits a direct algebraic interpretation in terms of the coefficient matrix C . For a two-qutrit pure state, the determinant of C is related to the eigenvalues of ρ_A through

$$\det(\rho_A) = |\det C|^2 = \lambda_1 \lambda_2 \lambda_3. \quad (12)$$

Related invariant-based descriptions of bipartite and multipartite quantum states have been studied from both nonlocal and algebraic perspectives [7–9].

The determinant thus vanishes identically for all rank-2 states and is nonzero only for rank-3 states as expected from invariant consideration [7]. This observation motivates the introduction of a determinant-based geometric invariant that quantifies genuinely three-level entanglement [7].

The symmetric polynomial description therefore provides a clear geometric picture of two-qutrit entanglement. While s_2 determines the strength of pairwise correlations [5, 6], s_3 distinguishes states with genuine three-level entanglement from those that effectively reduce to lower-dimensional subspaces. In the following section, this geometric insight is used to construct a normalized determinant-based invariant and to derive an analytic constraint relating it to the I-concurrence.

4 Determinant-Based Invariant and Analytic Constraint

The symmetric polynomial structure discussed in the previous section naturally motivates the definition of a geometric invariant that is sensitive to genuine three-level correlations. Since the third-order polynomial s_3 vanishes for all rank-2 states and is nonzero only for rank-3 states, it provides a natural basis for constructing such an invariant [7].

We define the normalized determinant-based geometric invariant as

$$G = 3\sqrt{3} \sqrt{s_3} = 3\sqrt{3} \sqrt{\lambda_1 \lambda_2 \lambda_3}. \quad (13)$$

The normalization factor $3\sqrt{3}$ is chosen such that G attains its maximum value unity for maximally entangled two-qutrit pure states, where $\lambda_1 = \lambda_2 = \lambda_3 = 1/3$ [1]. By construction, the invariant G vanishes identically for all rank-2 states and is strictly positive only for rank-3 states, thereby serving as a faithful indicator of genuine three-level entanglement.

The eigenvalues of the reduced density matrix ρ_A satisfy the characteristic equation

$$x^3 - x^2 + s_2 x - s_3 = 0, \quad (14)$$

whose roots are $\{\lambda_1, \lambda_2, \lambda_3\}$.

Requiring the eigenvalues to be real and non-negative implies that the discriminant of the cubic polynomial must be non-negative, which leads to the inequality

$$27s_3^2 \leq 4s_2^3. \quad (15)$$

This inequality follows from the requirement that the discriminant of the cubic characteristic polynomial be non-negative, ensuring that all eigenvalues of ρ_A are real and non-negative. Here s_2 and s_3 are the elementary symmetric polynomials defined earlier. Physical realizability of a two-qutrit pure state therefore requires all three roots of the characteristic equation to be real and non-negative, which imposes a constraint on the allowed values of s_2 and s_3 through the non-negativity of the discriminant [7].

Expressing the symmetric polynomials in terms of the entanglement measures I -concurrence C_I and the determinant-based invariant G using $s_2 = C_I^2/4$ and $s_3 = G^2/27$ [5, 6], the discriminant condition yields an explicit inequality relating the two invariants,

$$C_I^6 - C_I^4 - 72C_I^2G^2 + 432G^4 + 64G^2 \leq 0 \quad (16)$$

Although both the I -concurrence C_I and the determinant-based invariant G depend solely on the eigenvalues of the reduced density matrix, they capture distinct physical content: C_I quantifies pairwise coherence through second-order eigenvalue correlations, whereas G characterizes genuinely three-level entanglement via the third-order symmetric polynomial.

The resulting inequality delineates the physically admissible region of two-qutrit states in the (C_I, G) plane. States lying outside this region do not correspond to valid density matrices and are therefore unphysical. The boundary of the allowed region is obtained when the inequality is saturated, which corresponds to spectral degeneracy of the reduced density matrix, where two or more eigenvalues coincide [8].

As a result, the analytic constraint provides a complete geometric characterization of two-qutrit entanglement in terms of the I -concurrence and the determinant-based invariant, consistent with geometric approaches to entanglement classification [14]. The validity of this analytic constraint is further confirmed by numerical sampling of random two-qutrit pure states. For all sampled states, the corresponding values of C_I and G lie strictly within the region defined by the inequality, while the boundary is saturated only in cases of spectral degeneracy of the reduced density matrix.

The inequality further highlights the complementary roles of the two invariants. While the I -concurrence captures correlations associated with pairwise coherences [5, 6, 15], the invariant G quantifies genuinely three-level entanglement. Together, they provide a minimal and complete description of the entanglement geometry of two-qutrit pure states.

5 Optical Interpretation and Quantum Erasure

The geometric invariants introduced above admit a natural operational interpretation in the context of multi-path optical interferometry. In particular, a two-qutrit system can be mapped onto a three-path interferometer, where each qutrit basis state corresponds to a distinct propagation path. Within this framework, the reduced density matrix elements acquire direct physical meaning in terms of path populations and interference visibilities [11–13].

For a three-path interferometer with relative phase shifts $\{\phi_1, \phi_2, \phi_3\}$, the detected intensity can be written as

$$I(\phi_1, \phi_2, \phi_3) = \sum_i \rho_{ii} + 2\Re \sum_{i < j} e^{i(\phi_i - \phi_j)} \rho_{ij}. \quad (17)$$

Quantitative formulations of wave–particle duality have been extended to multi-path and multi-beam interferometers, which are particularly relevant for higher-dimensional systems [16, 17].

where the diagonal elements ρ_{ii} correspond to individual path intensities and the off-diagonal elements ρ_{ij} encode pairwise interference contributions. The exponential phase factors determine the positions of the interference fringes, while the real part gives rise to observable oscillations.

In this way, the coherence structure of the reduced density matrix is directly reflected in the interference pattern [11, 12, 16].

To analyze the effects of which-path information, we consider a marked three-path state of the form

$$|\Psi\rangle = \sum_{i=1}^3 c_i |\pi_i\rangle |\sigma_i\rangle, \quad (18)$$

where $|\pi_i\rangle$ denote the path states and $|\sigma_i\rangle$ represent the corresponding marker states [11, 18].

In a realistic interferometric setup, each path may be subject to an amplitude transmittance $t_i \geq 0$, yielding the effective state

$$|\Psi\rangle = \sum_{i=1}^3 \sqrt{t_i} c_i |\pi_i\rangle |\sigma_i\rangle. \quad (19)$$

In an erasure protocol, the marker subsystem is projected onto a chosen erasure state $|e\rangle$ [19, 20]. Defining the overlap amplitudes $\alpha_i = \langle e|\sigma_i\rangle$ and the corresponding intensities $\tau_i = |\alpha_i|^2$, the post-selected (unnormalized) path state becomes

$$|\psi_e\rangle = \sum_{i=1}^3 \sqrt{t_i} c_i \alpha_i |\pi_i\rangle. \quad (20)$$

The success probability of the erasure process is given by

$$P_e = \sum_{i=1}^3 |c_i|^2 t_i \tau_i, \quad (21)$$

and the normalized conditional path state follows straightforwardly.

The conditional predictability after erasure is determined by the path populations

$$p_i^{(\text{cond})} = \frac{|c_i|^2 t_i \tau_i}{\sum_k |c_k|^2 t_k \tau_k}, \quad (22)$$

which satisfy $\sum_i p_i^{(\text{cond})} = 1$. A suitable normalized measure of qutrit predictability is then defined as [13, 16]

$$P_{\text{cond}} = \sqrt{\frac{3}{2} \sum_{i=1}^3 \left(p_i^{(\text{cond})} - \frac{1}{3} \right)^2}, \quad (23)$$

generalizing the standard two-path predictability to three-path interferometry [12, 16, 17].

The recovered interference after erasure is quantified by the conditional visibility. Summing the contributions from all unordered path pairs yields

$$V_{\text{cond}} = \frac{\sum_{i < j} 2|c_i c_j| \sqrt{t_i t_j} \sqrt{\tau_i \tau_j}}{\sum_k |c_k|^2 t_k \tau_k}, \quad (24)$$

which captures the restoration of interference due to the erasure of which-path information [11, 13, 21].

Several complementary frameworks, ranging from coherence-based descriptions to delayed-choice and optimal tradeoff approaches, have been explored in the literature [22–27].

These expressions reduce to the corresponding ideal forms in the limit of unit transmittance and perfect erasure.

The determinant-based geometric invariant also acquires a simple operational modification in the presence of unequal transmittances [11, 12, 16]. Denoting by G the ideal invariant, the transmittance-weighted form reads [25, 28]

$$G_T = 3\sqrt{3} \sqrt{t_1 t_2 t_3} \sqrt{\lambda_1 \lambda_2 \lambda_3}. \quad (25)$$

The conditional quantities satisfy the extended complementarity relation [25, 29]

$$P_{\text{cond}}^2 + V_{\text{cond}}^2 + G_T^2 \leq 1. \quad (26)$$

The role of entanglement in constraining wave–particle duality relations has been explicitly analyzed in interferometric settings [24–26]. This inequality expresses a three-way tradeoff between which-path information, recovered two-path coherence, and genuine three-level geometric coherence [13, 28, 29].

The relevance of multi-level coherence and entanglement extends to practical quantum information protocols implemented on current quantum hardware [30].

6 Numerical Demonstrations

In this section, we present numerical simulations to illustrate the analytic constraints and operational relations derived in the previous sections. The numerical results are intended to provide explicit confirmation of the geometric structure of two-qutrit entanglement and its operational manifestation in quantum erasure protocols [11, 13, 29].

Random two-qutrit pure states were generated by sampling complex coefficient matrices C subject to normalization. For each realization, the reduced density matrix $\rho_A = CC^\dagger$ was constructed and its eigenvalues were computed. The corresponding I-concurrence C_I and determinant-based invariant G were then evaluated using the definitions introduced earlier [5, 6]. Only physically valid states satisfying the analytic constraint of Section 4 were retained.

Figure 1 shows the distribution of two-qutrit states in the (C_I, G) plane. Rank-2 states lie entirely on the line $G = 0$, while rank-3 states populate the interior of the allowed region bounded by the analytic inequality corresponding to spectral degeneracy of the reduced density matrix. The numerical points are seen to lie strictly within this boundary, confirming the validity of the analytic constraint.

We next illustrate the behavior of conditional visibility and predictability in the two-qutrit quantum erasure protocol. Figure 2 displays the variation of the conditional visibility V_{cond} and predictability P_{cond} as functions of the transmittance parameter τ , demonstrating the expected complementary behavior [11, 12, 16, 28].

The numerical results are fully consistent with the extended complementarity relation derived in Section 5. Deviations from saturation arise from nonidealities such as unequal transmittances or partial erasure, while the overall tradeoff structure remains intact. These simulations therefore provide direct numerical support for the unified geometric and operational framework developed in this work.

7 Conclusion

In this work, we have presented a unified geometric and operational description of entanglement in bipartite two-qutrit pure states. By analyzing the eigenvalue structure of the reduced density matrix

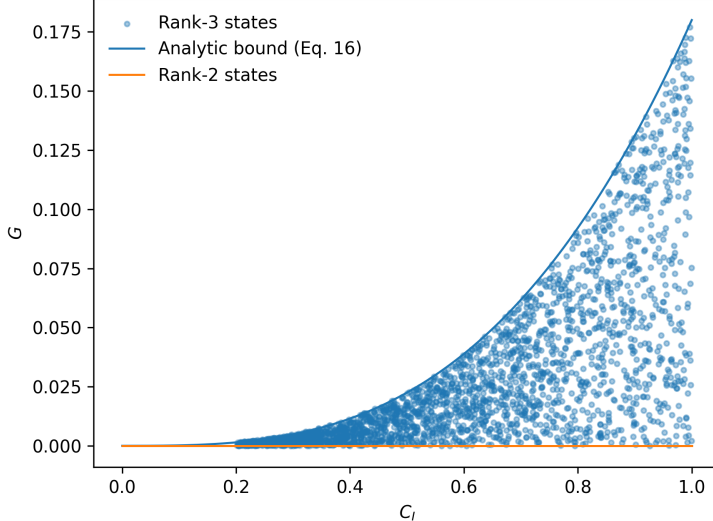


Figure 1: Scatter plot of randomly generated two-qutrit pure states in the (C_I, G) plane. Rank-2 states lie on the line $G = 0$, while rank-3 states populate the interior of the physically allowed region. The solid curve denotes the analytic boundary obtained by saturating Eq. (16).

through symmetric polynomials, we have clearly separated pairwise correlations from genuinely three-level correlations [1, 5, 6]. This approach provides a transparent geometric framework for understanding higher-dimensional entanglement.

We have shown that the determinant of the coefficient matrix defines a natural, rank-sensitive geometric invariant that vanishes for all rank-2 states and is nonzero only for genuine rank-3 entanglement. An explicit analytic constraint relating this determinant-based invariant to the I-concurrence was derived, thereby identifying the physically accessible region of two-qutrit states in invariant space. This constraint offers a complete geometric characterization of two-qutrit entanglement in terms of two complementary quantities.

An operational interpretation of the geometric invariants was established through a mapping to three-path optical interferometry. Within this framework, we derived expressions for conditional visibility and predictability in a qutrit quantum erasure protocol, including the effects of unequal path transmittances. The resulting extended complementarity relation reveals a three-way tradeoff between which-path information, recovered two-path coherence, and genuine three-level geometric coherence[11–13, 16].

The combination of analytic results and numerical demonstrations confirms the consistency and robustness of the proposed framework. The geometric and operational connections developed here provide new insight into the structure of higher-dimensional entanglement and its observable manifestations. Future work may explore extensions to mixed states, higher-dimensional systems, or experimental implementations in multi-path interferometric platforms. The present results are consistent with broader efforts to understand the role of coherence and entanglement in quantum information theory[22, 29].

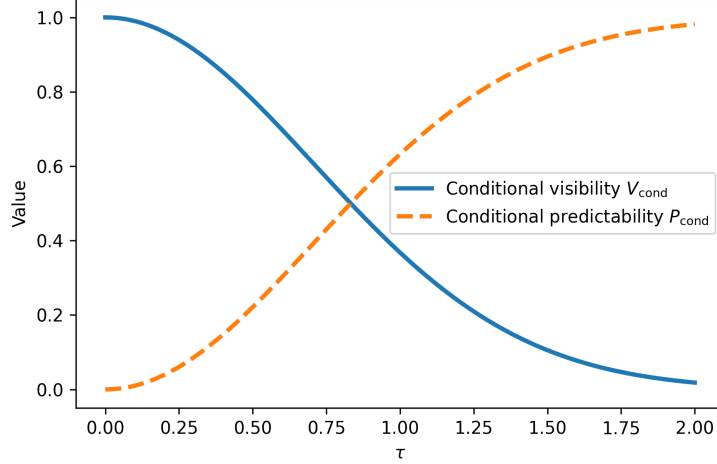


Figure 2: Conditional visibility V_{cond} and conditional predictability P_{cond} as functions of the erasure parameter τ . The tradeoff between the two quantities demonstrates wave–particle complementarity in the qutrit quantum erasure scheme.

References

- [1] R. Horodecki, P. Horodecki, M. Horodecki, and K. Horodecki. Quantum entanglement. *Reviews of Modern Physics*, 81:865–942, 2009.
- [2] H. Bechmann-Pasquinucci and A. Peres. Quantum cryptography with 3-state systems. *Physical Review Letters*, 85:3313–3316, 2000.
- [3] D. Kaszlikowski, P. Gnaciński, M. Żukowski, W. Miklaszewski, and A. Zeilinger. Violations of local realism by two entangled n-dimensional systems. *Physical Review Letters*, 85:4418–4421, 2000.
- [4] D. Collins, N. Gisin, N. Linden, S. Massar, and S. Popescu. Bell inequalities for arbitrarily high-dimensional systems. *Physical Review Letters*, 88:040404, 2002.
- [5] P. Rungta, V. Bužek, C. M. Caves, M. Hillery, and G. J. Milburn. Universal state inversion and concurrence in arbitrary dimensions. *Physical Review A*, 64:042315, 2001.
- [6] P. Rungta and C. M. Caves. Concurrence-based entanglement measures for isotropic states. *Physical Review A*, 67:012307, 2003.
- [7] S. Albeverio and S.-M. Fei. A note on invariants and entanglement measures. *Journal of Optics B: Quantum and Semiclassical Optics*, 3:223–227, 2001.
- [8] N. Linden, S. Popescu, and A. Sudbery. Nonlocal parameters for multiparticle density matrices. *Physical Review Letters*, 83:243–247, 1999.
- [9] P. D. Jarvis. The mixed two-qutrit system: local unitary invariants, entanglement monotones, and the slocc group $\text{sl}(3,\mathbb{C})$. *Journal of Physics A: Mathematical and Theoretical*, 47(21):215302, 2014.
- [10] Andreas Osterloh. Sl-invariant extension of the concurrence to higher local hilbert-space dimensions. *Journal of Physics A: Mathematical and Theoretical*, 48(6):065303, 2015.

- [11] B.-G. Englert. Fringe visibility and which-way information: An inequality. *Physical Review Letters*, 77:2154–2157, 1996.
- [12] S. Dürr. Quantitative wave-particle duality in multibeam interferometers. *Physical Review A*, 64:042113, 2001.
- [13] Tabish Qureshi. Predictability, distinguishability, and entanglement. *Optics Letters*, 46(3):492–495, 2021.
- [14] Soumik Mahanti, Sagnik Dutta, and Prasanta K. Panigrahi. Classification and quantification of entanglement through wedge product and geometry. *Physica Scripta*, 98(8):085103, 2023.
- [15] Abhinash Kumar Roy, Neha Pathania, Nitish Kumar Chandra, Prasanta K. Panigrahi, and Tabish Qureshi. Coherence, path-predictability, and i-concurrence: A triality. *Physical Review A*, 105(3):032209, 2022.
- [16] M. Jakob and J. A. Bergou. Quantitative complementarity relations in bipartite systems. *Optics Communications*, 283:827–833, 2010.
- [17] Tabish Qureshi and Mohd Asad Siddiqui. Wave-particle duality in n-path interference. *Annals of Physics*, 385:598–604, 2017.
- [18] D. M. Greenberger and A. Yasin. Simultaneous wave and particle knowledge in a neutron interferometer. *Physics Letters A*, 128:391–394, 1988.
- [19] M. O. Scully, B.-G. Englert, and H. Walther. Quantum optical tests of complementarity. *Nature*, 351:111–116, 1991.
- [20] P. D. D. Schwindt, P. G. Kwiat, and B.-G. Englert. Quantitative wave-particle duality and non-erasing quantum eraser. *Physical Review A*, 60:4285–4290, 1999.
- [21] Naveed Ahmad Shah and Tabish Qureshi. Quantum eraser for three-slit interference. *Pramana – Journal of Physics*, 89:51, 2017.
- [22] T. Baumgratz, M. Cramer, and M. B. Plenio. Quantifying coherence. *Physical Review Letters*, 113:140401, 2014.
- [23] Y.-H. Kim, R. Yu, S. P. Kulik, Y. Shih, and M. O. Scully. A delayed-choice quantum eraser. *Physical Review Letters*, 84:1–5, 2000.
- [24] G. Jaeger, A. Shimony, and L. Vaidman. Two interferometric complementarities. *Physical Review A*, 51:54–67, 1995.
- [25] P. J. Coles, J. Kaniewski, and S. Wehner. Entropic wave-particle duality relations and the uncertainty principle. *Physical Review A*, 89:022112, 2014.
- [26] S. Dürr and G. Rempe. Can wave-particle duality be based on the uncertainty relation? *American Journal of Physics*, 68(11):1021–1024, 2000.
- [27] E. Bagan, J. A. Bergou, S. S. Cottrell, and M. Hillery. Relations between coherence and path information. *Physical Review Letters*, 116:160406, 2016.
- [28] X.-F. Qian, A. N. Vamivakas, and J. H. Eberly. Entanglement limits duality and vice versa. *Optica*, 5:942–947, 2018.

- [29] M. N. Bera, T. Qureshi, M. A. Siddiqui, and A. K. Pati. Duality of quantum coherence and path distinguishability. *Physical Review A*, 92:012118, 2015.
- [30] D. Joy, M. Sabir, B. K. Behera, and P. K. Panigrahi. Implementation of quantum secret sharing and quantum binary voting protocol in the ibm quantum computer. *Quantum Information Processing*, 19:33, 2020.